J Comp Physiol A (2002) 188: 739–752
DOI 10.1007/s00359-002-0363-1

REVIEW

Andrew S. French · Päivi H. Torkkeli
Ernst-August Seyfarth

From stress and strain to spikes: mechanotransduction in spider slit sensilla

Received: 22 July 2002 / Revised: 21 September 2002 / Accepted: 23 September 2002 / Published online: 31 October 2002

Abstract This review focuses on the structure and function of a single mechanoreceptor organ in the cuticle of spiders. Knowledge emerging from the study of this organ promises to yield general principles that can be applied to mechanosensation in a wide range of animal systems. The lyriform slit sense organ on the antero-lateral leg patella of the spider *Cupiennius salei* is unusual in possessing large sensory neurons, whose cell bodies are close to the sites of sensory transduction, and accessible to intracellular recording during mechanotransduction. This situation, combined with recent technical developments, has made it possible to observe and experiment with all the major stages of mechanosensation. Important findings include the approximate size, number and ionic selectivity of the ion channels responsible for mechanotransduction, the types of voltage-activated ion channels responsible for action potential encoding, and the mechanisms controlling the dynamic properties of transduction and encoding. Most recently, a complex efferent system for peripheral modulation of mechanosensation has been discovered and partially characterized. Much remains to be learned about mechanosensation, but the lyriform slit sense organ system continues to offer important opportunities to advance our understanding of this crucial sense.

Keywords Encoding · Mechanoreception · Noise analysis · Peripheral synapses · Sensory adaptation

Abbreviations *VS-3* lyriform organ on antero-lateral leg patella; · *TTX* tetrodotoxin

A.S. French (✉) · P.H. Torkkeli
Department of Physiology and Biophysics,
Dalhousie University, Halifax, NS, B3H 4H7, Canada
E-mail: andrew.french@dal.ca
Tel.: +1-902-4941302
Fax: +1-902-4942050

E.-A. Seyfarth
Zoologisches Institut, J.W. Goethe-Universität,
Siesmayerstraße 70, 60054 Frankfurt am Main, Germany

Introduction

Mechanosensation is a vitally important function in animals from unicellular organisms to the most complex vertebrates, but its fundamental mechanisms have been difficult to unravel, particularly because of the small size and complex morphology of many mechanoreceptor endings. Arthropods possess an important class of mechanoreceptors, the cuticular or type I receptors, that have their somata in the periphery, close to the sites of mechanotransduction and action potential initiation (McIver 1985; French 1988). Even these sensory neurons present formidable experimental difficulties, including small size, inaccessibility and the problem of providing mechanical stimulation while trying simultaneously to record electrical events in the membranes.

Spiders have cuticular mechanoreceptors called slit sense organs that are widely distributed in the exoskeleton (Barth and Libera 1970; Barth 1985, 2001). These organs detect mechanical events in the cuticle, primarily strains imposed by normal movements and vibrations due to predators, prey and mates. Slit sense organs have provided important experimental preparations for research into mechanosensation because of the following advantages compared to many other invertebrate cuticular mechanoreceptors: (1) their mechanical structures, while still complex, are approximately two-dimensional and more amenable to analysis and stimulation; (2) preparations have been developed that allow simultaneous mechanical stimulation and stable intracellular recording, including voltage-clamp; (3) the ability to detach the neurons from the cuticle has facilitated investigation of their voltage-activated conductances; and (4) the complex efferent innervation that has recently been discovered promises to shed new light on mechanisms of peripheral and central modulation of sensory systems.

Here, we review major findings that have emerged from research on slit sense organs at each stage of the

mechanotransduction process, from mechanical stimulation to the generation of action potentials.

Basic functional anatomy of slit sensilla

Structure

Slit sense organs are cuticular mechanoreceptors characteristic to arachnids, such as spiders, scorpions, and harvestmen. Each cuticular slit is provided with two mechanosensitive neurons, which act as biological strain sensors in the relatively hard exoskeleton. Barth and Libera (1970) mapped and classified the organs in the wandering spider *Cupiennius salei* Keys (Ctenidae) where they occur in three different configurations: (1) more than 1,500 isolated single slits, ranging from 10 to 150 μm in length, are distributed over the entire body surface; (2) groups of individual slits gathered at particular sites in the exoskeleton but spaced 100 μm apart; and (3) more than 140 compound organs comprising 2–29 slits closely arranged in parallel. The latter are also known as "lyriform organs" because the graduated arrangement of their slits resembles the shape of a lyre. The lengths of their cuticular slits vary from a few to 200 μm and are not correlated with the sizes of the associated sensory neurons. Lyriform organs are confined to body appendages and are particularly prominent near the joints of walking legs. In this review we focus on lyriform organ VS-3 (nomenclature of Barth and Libera 1970), which is located on the anterior side of the leg patella and consists of 7 or 8 slits (Fig. 1A).

The basic anatomy and ultrastructure of all slit sense organs are essentially the same, as first detailed by Barth (1971) who also proposed functional roles for the various fine-structural elements. In VS-3, the two bipolar neurons associated with each slit have relatively large fusiform somata (Fig. 1B) ranging from 20 μm to more than 100 μm in diameter (Fabian and Seyfarth 1997).

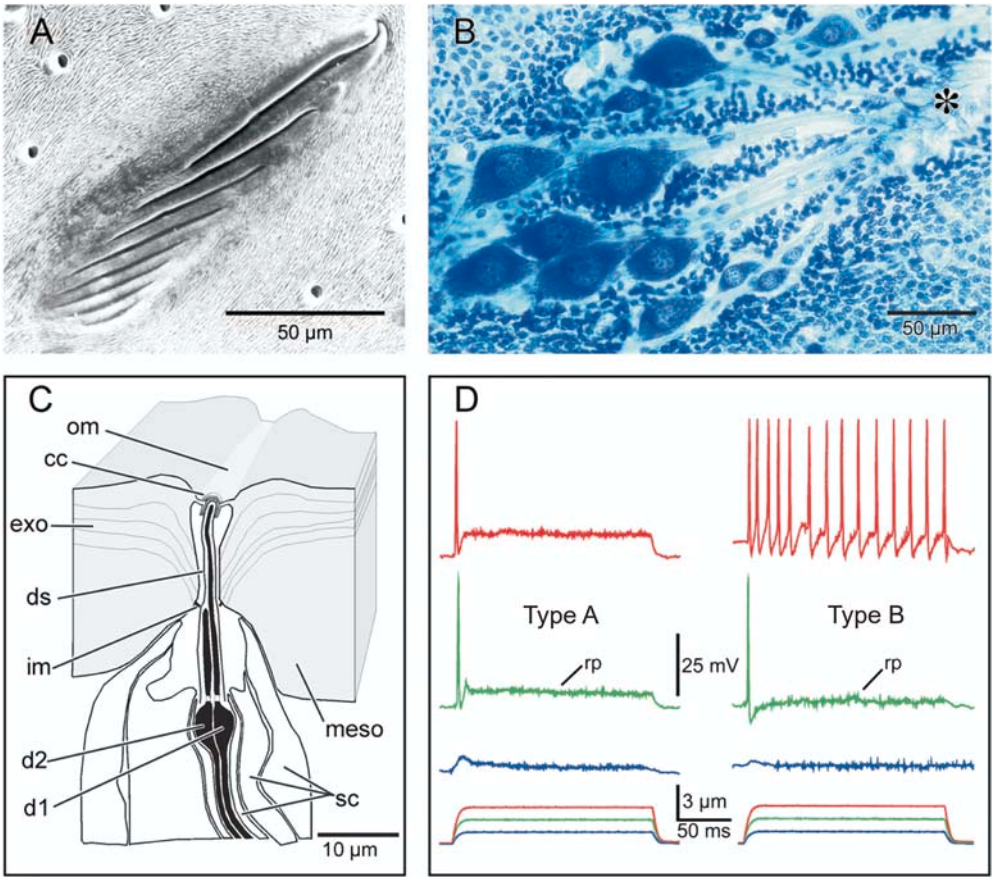

Fig. 1A–D Anatomy and basic electrophysiological responses of lyriform slit sense organ VS-3. **A** External cuticular features; the scanning electron micrograph shows eight cuticular slits. Sockets of plucked sensory hairs surround the lyriform organ. **B** Inside view of a methylene blue-stained VS-3 organ reveals pairs of fusiform neuronal somata and their dendrites extending towards the slit region (*asterisk*, *upper right*). The smaller globular cells are hemocytes and pigment cells attached to the hypodermis. **C** Schematized cross section through a single slit and its associated pair of mechanosensory dendrites. Only the distal dendritic regions are shown; the neuronal somata lie further proximally (drawing modified from Barth 1971). *om* outer membrane, *cc* coupling cylinder, *d1*, *d2* dendrites, *ds* dendritic sheath, *exo* exocuticle, *im* inner membrane, *meso* mesocuticle, *sc* glial sheath cells. **D** Responses to step mechanical stimuli of increasing amplitude (*bottom traces*) in a type A neuron (*left*) and a type B neuron (*right*); intracellular recordings. Small mechanical stimuli produced a graded, depolarizing receptor potential (*rp*, *blue*) and only one action potential (*green*), but larger stimulus amplitudes (>3 μm; *red*) revealed the difference in adaptation behavior between the two neurons. Modified from Höger and Seyfarth (2001)

The sensory dendrites are wrapped in glial sheaths, and their tips are attached to specialized cuticular structures within the slits. The tip of one dendrite in each neuron pair (d1) fully extends through the slit and is coupled to an outer membrane via a coupling cylinder (''cc'' in Fig. 1C); the other dendrite (d2) is shorter and terminates close to an inner membrane at the slit entrance. The dendrite tips are surrounded by an extracellular space known as the ''receptor lymph space''. Both dendrites are ciliated; the tips contain a ''tubular body'', i.e., a region of densely packed microtubules. A cutaway view of this anatomical arrangement is shown in Fig. 1C. Mechanotransduction probably happens only at the dendrite tips, in the region concealed by slit cuticle, because mechanical stimulation of more proximal dendrite regions did not excite the neurons (Höger and Seyfarth 2001).

The neural somata, proximal dendrites and axons are embedded in the hypodermis, a thin layer of epidermal tissue that underlies the exoskeleton. In the case of VS-3, a piece of cuticle can be dissected from the patella, containing the cuticular slit structures and all neuronal parts, dendrites, somata, and initial axon segments. In addition, the hypodermis can be separated from the cuticle, yielding a ''hypodermis preparation'' that includes the neuronal parts except the tips of the dendrites, which are lost during detachment. Both preparations are suitable for intracellular recordings. The hypodermis preparation allows rapid application and exchange of solutions for pharmacological experiments.

Mechanical stimuli and basic electrophysiological response

Slit sense organs detect minute mechanical strains in the exoskeleton. In physical terms, strain is the consequence of applying stress to a material, and in spider cuticle, such strains result from loads and stress acting on the exoskeleton. The effective stimulus leading to electrical activity in the sensory neurons is compressive (that is by definition negative) strain in the plane of the exocuticle that reaches the slits perpendicular to their long axis (Barth 1972a, 1972b). As detailed by Barth (1985, 2001), slit compression induces mono-axial compressional forces that cause non-uniform deformation of the dendrite tips. In the case of the longer dendrite d1, the forces act via the coupling cylinder, while the shorter dendrite d2 apparently lacks such a firm coupling structure (Fig. 1C). Dilation of the slits by positive mechanical strains is not effective in exciting the sensory neurons.

Both neurons innervating each slit are mechanically sensitive and produce a graded receptor potential (''rp'' in Fig. 1D) when the slit is compressed via a stimulus probe placed against the slit cuticle (Juusola et al. 1994; Höger et al. 1997). Supra-threshold stimuli cause both neurons to generate action potentials, but their responses to sustained mechanical or electrical stimuli have different time-courses: one (type A) adapts rapidly and produces only one to two action potentials, while its partner (type B) generates bursts (Fig. 1D) (Seyfarth and French 1994). The two neuron types are also chemically different. Both were immunoreactive to the ACh-synthesizing enzyme choline acetyltransferase (ChAT) and probably use ACh as a neurotransmitter, but only type A neurons were strongly labeled for histamine and the ACh-degrading enzyme acetylcholine esterase (AChE) (Fabian and Seyfarth 1997).

The mechanical sensitivity of slit sense organs depends on their deformability, which in turn depends on anatomical and biomechanical factors such as slit length, shape of the covering membrane, position of the dendrites along the length of the slit, and exact orientation of the slits in the exoskeleton with respect to the compressive forces. In the case of lyriform organs, the sensitivity of each slit is greatly affected by its relative position within the compound organ. The biomechanical parameters and their functional consequences are reviewed and discussed in detail by Barth (1985, 2001).

Efferent neurons and synapses

An interesting feature of all cuticular sense organs in arachnids is that they receive numerous chemical synaptic contacts in the periphery. First discovered by Foelix (1975) in the sensory leg nerves of whip spiders and harvestmen, detailed studies have recently been performed in the spider VS-3 organ. A monoclonal antibody against the presynaptic vesicle protein synapsin revealed punctate immunoreactivity in wholemount preparations of VS-3 (Fabian-Fine et al. 1999a, 1999b). Immunoreactive puncta were linearly arranged along several fine, varicose fibers and distributed across the dendrites, somata, and axons of all neurons (Fig. 2A, B), with most presynaptic sites at the initial axon segments. Fine-structural analysis and 3-D reconstruction of ultrathin serial sections showed that several fine fibers and numerous chemical synapses (with several vesicle types) were present at the sensory neurons and their surrounding glial sheaths. An example is shown in Fig. 2C. Electron microscope examination of anti-synapsin stained VS-3 preparations confirmed that reaction product was associated with synaptic vesicles. Moreover, sectioning the leg nerve led to rapid degeneration (within 4 h) of most fine fiber profiles, indicating that the fibers originated in the central nervous system, i.e., were efferents (Fabian-Fine et al. 1999b). There were no lateral synaptic contacts directly between the sensory neurons, but numerous contacts among the fine fibers themselves (Fabian-Fine et al. 2002; see also Panek et al. 2002). These anatomical results suggested that the peripheral synaptic contacts originate from efferents that could exert complex centrifugal control of mechanosensory activities. Identification of neurotransmitter candidates at these synapses, possible functions, and recent studies of peripheral GABAergic inhibition of VS-3 neurons are discussed further below.

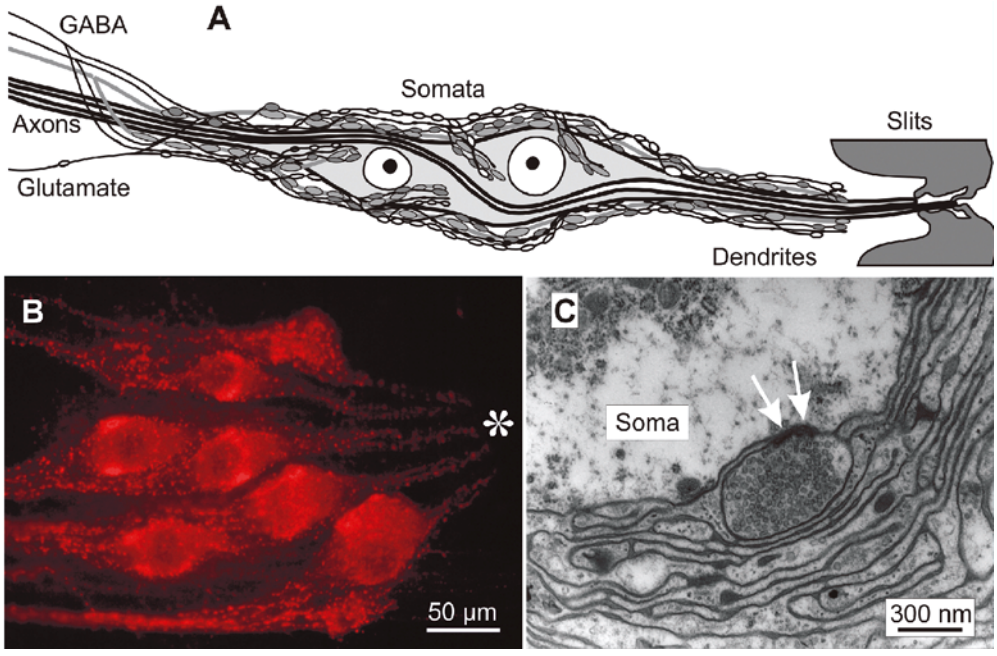

Fig. 2A–C The VS-3 organ receives peripheral synaptic contacts. **A** Schematic diagram showing the distribution of efferent endings surrounding a pair of neurons innervating one slit. Several fine fibers run parallel to the bipolar neurons and form numerous synapses onto their initial axon segments, somata, and dendrites, as well as onto surrounding glial cells and with each other. At least three types of efferent fibers show immunoreactivity to GABA, and at least one efferent fiber shows immunoreactivity to glutamate. **B** Immunofluorescent labeling of VS-3 neurons with a monoclonal antibody against the vesicle protein synapsin. Immunoreactive puncta are linearly arranged and distributed across all neuronal segments, dendrites (*right*), somata (*center*), and initial axon segments (*left*). *Asterisk*: dendrite tips extending towards the slit region. Patchy fluorescence inside somata is due to autofluorescence of lipofuscin deposits. **C** Electron micrograph of a fine efferent fiber (*center*) synapsing onto the soma of a sensory neuron; *arrows*: electron-dense active zone. Micrographs taken by Ruth Fabian-Fine

Mechano-electrical transduction

The fundamental step in mechanotransduction is when a mechanical stimulus causes an electric current to flow across a cell membrane. Up to about 50 years ago, simple mechanical disruption of a cell membrane was thought to allow current to flow under the driving force of the membrane potential, but it now seems certain that specialized ion channels, often called mechanically activated channels, are strategically located in mechanoreceptor neurons, close to the sites of mechanical stimulation. Single mechanically activated channels have been characterized in many cells (Morris 2001) but there are still no single-channel recordings from sensory neurons that can be clearly identified as the channels responsible for sensory transduction.

The ultrastructure of VS-3 suggests that sensory transduction occurs at the tips of the dendrites (Fig. 1C) and this was supported by the observation that punctate stimulation of the dendrites proximal to the slits did not cause transduction (Höger and Seyfarth 2001). The dendrites contain dense microtubules, but disruption of these by prolonged stimulation in the presence of colchicine did not eliminate the receptor potential. This echoes similar findings in insect cuticular mechanoreceptors (reviewed in French 1988), and makes it unlikely that microtubules are involved in sensory transduction.

Mechanical stimulation of the slits in VS-3 leads to a depolarizing receptor potential that causes action potentials if it is large enough (Juusola et al. 1994) (Figs. 1D, 3). Single-electrode voltage clamp of the neurons is possible through relatively high-resistance electrodes (~60 MΩ) and a high-frequency switching amplifier (Polder and Swandulla 2001). Recording quality can be significantly enhanced by coating the electrode tip (Juusola et al. 1997). Voltage clamp and the addition of tetrodotoxin (TTX) to block voltage-activated Na^+ current revealed an inward receptor current during mechanical stimulation at the resting potential of about –70 mV. Part of the receptor current adapted over a period of about 100 ms but another part was persistent for much longer (Fig. 3A, B).

At more positive potentials the receptor current decreased and was undetectable at ~100 mV, but did not reverse direction (Fig. 3C). Since extracellular solutions are usually rich in Na^+ and intracellular solutions in K^+, this would normally mean that the ion channels carrying the receptor current are strongly selective for Na^+. However, the receptor lymph space surrounding the dendritic tips of arthropod cuticular sensilla may have different ionic composition and electrical potential to the normal extracellular space (French 1988). In slit sensilla there is evidence from X-ray microanalysis (Rick and Pawel 1976) and ion-sensitive electrodes (Grünert and Gnatzy 1987) that

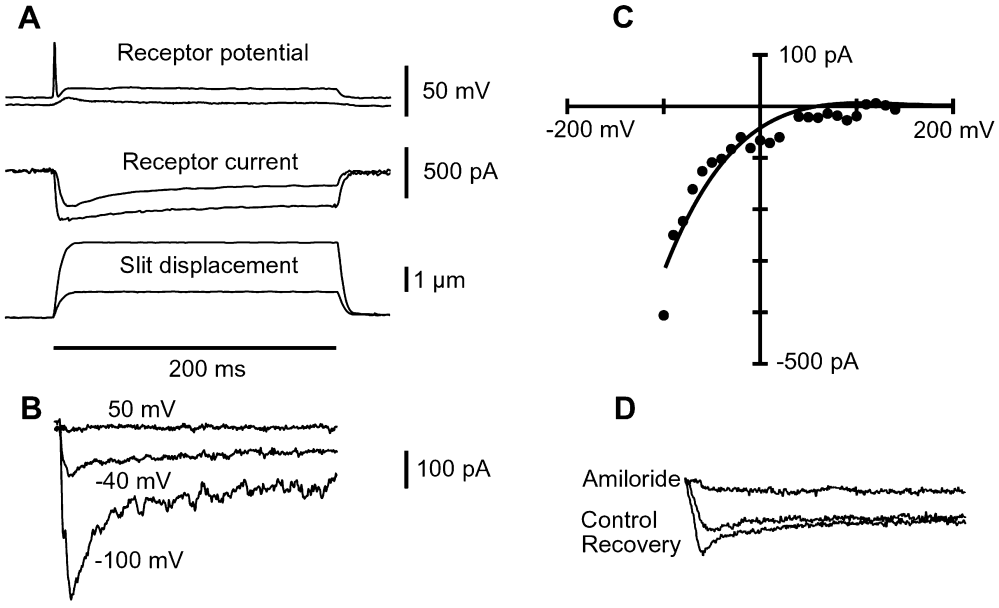

Fig. 3A–D Ionic selectivity and blockade of the mechanically-activated ion channels in VS-3 neurons observed by intracellular recording. **A** Slit displacement produced a receptor potential in a type A neuron that was detectable at 1 µm and large enough to produce an action potential at 3 µm (*top*). Similar displacements under voltage-clamp conditions revealed inward receptor currents flowing through the mechanically-activated ion channels (*middle*). **B**, **C** Receptor current increased as the cell membrane potential was hyperpolarized but failed to reverse at large positive potentials, indicating that the channels are highly selective for Na^+. The *solid line* is the fitted Goldman-Hodgkin-Katz current equation for Na^+. **D** Receptor current was reversibly reduced by the Na^+ channel blocker amiloride. Modified from Höger et al. (1997)

the lymph space Na^+ concentration is at least the same as the extracellular fluid, and there is no evidence for potential difference (Seyfarth et al. 1982; Grünert and Gnatzy 1987); hence the voltage-clamp data are consistent with channels that are highly selective for Na^+. Fitting the Goldman-Hodgkin-Katz current equation (Hille 2001) to the data gave a conductance of ~4.5 nS for the fully open channels.

Consistent with Na^+ selectivity, the receptor current was blocked by replacing external Na^+ with choline, or other cations, except Li^+, which gave ~50% of the Na^+ current. The current was also suppressed by the epithelial Na^+ channel blocker amiloride (Fig. 3D) and by Gd^{3+}, which blocks many mechanically activated channels, although not specifically (Yang and Sachs 1989).

Receptor potential adaptation

The receptor current and potential decay with time after a step movement (Fig. 3A), but the cause is not yet understood. Two possibilities are mechanical, such as viscoelastic behavior in the coupling from the slits to the sensory dendrite, and time-dependent behavior of the mechanically-activated channels themselves, but there is no convincing evidence for or against either possibility. Questions that arise immediately are whether adaptation of the receptor current contributes significantly to the overall adaptation of the action potential firing, and whether differences in receptor current adaptation contribute to the different firing patterns of type A and type B neurons?

The receptor potential adapted more rapidly in type A than in type B neurons (Fig. 4C, D), but there was no significant difference in the amplitude of adaptation, and the difference in time course was significant but not large (Juusola and French 1998). Most important, type A and type B firing patterns were seen clearly with direct electrical depolarization of the neurons (Fig. 4A, B), so they are independent of receptor current adaptation. The function of the receptor current adaptation remains enigmatic, although it probably makes a small contribution to the overall time course of receptor adaptation.

Receptor channel properties

Beyond their ionic selectivity and activation by mechanical stimuli, what do we know about the receptor channels? Single-channel recordings are not practicable with current technology, given their probable location at the tip of the sensory dendrite and the extensive glial wrappings of the neurons. One approach is to measure the variance, or noise, of the receptor current to estimate the single channel conductance and number of channels (Traynelis and Jaramillo 1998). This approach requires measurements over a range of different current amplitudes, which is made possible by the natural adaptation of the receptor current (Fig. 5A). For a single group of identical ion channels, the total variance, σ^2, of the current flowing through a membrane is given by:

$$\sigma^2 = \sigma_0^2 + I(V - E)\gamma - I^2/N \quad (1)$$

where σ_0^2 is the background variance due to other sources, I is total membrane current, V is the voltage

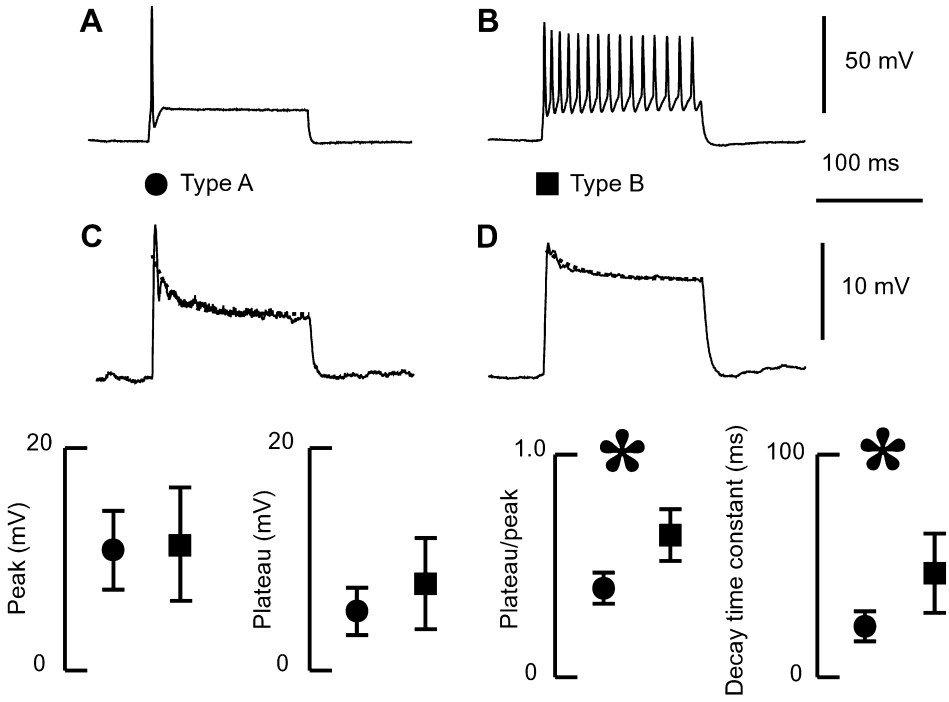

Fig. 4A–D Time dependence of receptor potential and action potential firing in VS-3 neurons. **A**, **B** Type A and type B firing patterns were shown by injecting 1 nA depolarizing currents intracellularly, demonstrating that the different firing patterns are controlled by events after the receptor potential. **C**, **D** Mechanical stimulation of the same two neurons under current-clamp when tetrodotoxin (TTX) was added to the bath solution showed adapting receptor potentials that were approximated by exponential decays (*superimposed dotted lines*). Mean values and standard deviations from 56 type A and 41 type B neurons (*lower*) showed that peak and plateau receptor potentials were similar in the two neuron types, but type A neurons had more rapidly adapting receptor potentials (*asterisks*: $P < 0.05$, Student's two-tailed *t*-test). However, this is clearly not the major reason for the difference between type A and type B neuronal firing patterns. Modified from Juusola and French (1998)

across the membrane, E is the equilibrium potential of the ions flowing through the channel, γ is the single-channel conductance, and N is the number of channels in the membrane. Figure 5B shows Eq. 1 fitted to the receptor current in a VS-3 neuron during adaptation to a step deformation of a slit. Similar measurements from 75 neurons gave mean values of $\gamma = 7.5$ pS and $N = 250$ channels. These data agree well with the small number of similar estimates from other mechanoreceptors (Höger and French 1999a) and indicate that transduction involves a relatively small number of specialized ion channels with low single-channel conductance. However, the total conductance of the open channels is more than adequate to depolarize the cells to the threshold for action potential production.

Given the single-channel conductance and number of channels, the open probability of the receptor channels can be calculated from:

$$\mathrm{Po} = I/\{N(V-E)\gamma\} \quad (2)$$

Application of Eq. 2 to the VS-3 organ data indicated that the channels are fully open at the start of a strong mechanical stimulus but decline to an open probability of about 0.2 after 60 s (Fig. 5A).

Another important property of receptor channels is their temperature sensitivity. Mechanotransduction is generally more thermally sensitive than would be predicted from simple ion channel conductance in a range of vertebrate and invertebrate receptors (reviewed in Höger and French 1999b). The VS-3 organ provided the first direct measure of receptor current temperature sensitivity and the data were well fitted by the Arrhenius equation (Fig. 5C, D) with a mean activation energy of 23 kcal mol^{-1} (97 kJ mol^{-1} or $Q_{10} = 3.2$). This is the highest activation energy measured for mechanotransduction, although close to measurements in other systems (Höger and French 1999b). It confirms the general finding that mechanotransduction involves a significant energy barrier, comparable to the energy required to break a covalent chemical bond.

Action potential initiation, encoding and adaptation

Action potentials in VS-3 neurons are driven by voltage-activated, TTX-sensitive Na^+ channels. Replacement of extracellular Na^+ with choline or application of TTX completely and reversibly blocked the production of action potentials (Fig. 6B, C). Complete characterization of this Na^+ current by voltage clamp proved difficult because it is fast compared with the temporal resolution of a switching clamp and the K^+ currents cannot be completely blocked (see below). However, reduction of the extracellular Na^+ concentration to

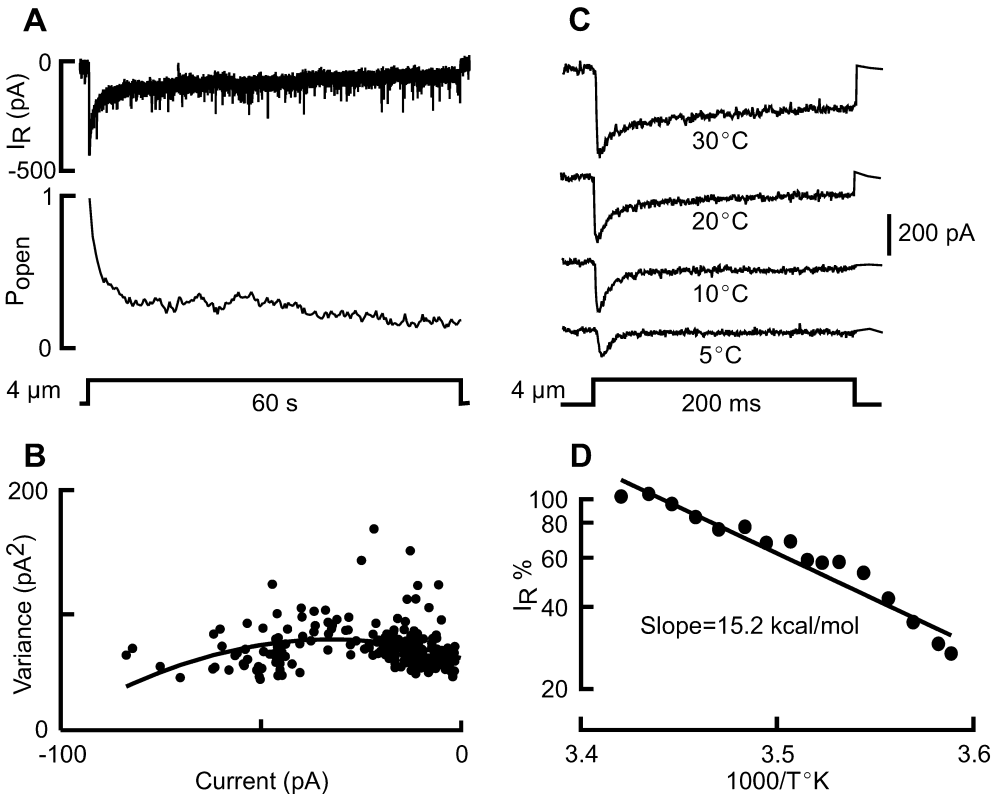

Fig. 5A–D The receptor current in VS-3 neurons is carried by relative small mechanically activated channels with high thermal activation energy. **A** Receptor current decayed following a step displacement due to a drop in the open probability of the mechanically-activated channels. **B** Receptor current variance had a parabolic dependence on current amplitude that was fitted by Eq. 1 with average values of 250 single channels of 7.5 pS conductance. **C** Receptor current increased strongly with temperature. **D** Temperature dependence was fitted by the Arrhenius equation, giving a mean activation energy of 23 kcal mol^{-1} ($Q_{10} = 3.2$), indicating that mechanotransduction involves a large thermal energy barrier. Modified from Höger and French (1999a, 1999b)

about 50% of normal allowed the voltage clamp to operate effectively, and subtraction of currents before and after TTX application revealed the Na^+ current (Fig. 6A). Further details of the experimental procedures and important properties of the voltage-activated Na^+ channels are described below.

The site of action potential initiation in arthropod cuticular receptors has caused considerable speculation (French 1988; Seyfarth et al. 1995). Although neuronal somata are relatively close to the sensory endings, the dendrites are often long and thin enough to attenuate a decrementally conducted receptor current. Most investigations have used extracellular stimulation and recording to explore this question. In VS-3 neurons the somata support overshooting action potentials, and combined mechanical and extracellular electrical recordings suggested that the sensory dendrites are also excitable (Seyfarth et al. 1982).

SP19 is a highly conserved, 19 amino acid sequence found in the intracellular segment of the voltage-activated Na^+ channel, and is probably part of the inactivation gate (Vassilev et al. 1989). Antibodies against the SP19 sequence stained all the major regions of VS-3 neurons (Fig. 6D), and some surrounding glial cells. Immuno-gold labeling, followed by electron microscopy, showed that Na^+ channel density is similar in the sensory dendrite and axonal regions, and about twice as high as in the somata (Seyfarth et al. 1995). These data support the idea that action potentials originate at the tips of the sensory dendrites and propagate through the somata, as originally suggested by extracellular experiments (Seyfarth et al. 1982).

Voltage-activated ion channels in type A and type B neurons

The small difference in receptor potential adaptation could not explain the difference in the firing behaviors of the type A and type B neurons. In addition, electrical stimulation produced the same differences in firing patterns between the neurons as mechanical stimulation, suggesting that voltage-activated conductances define action potential adaptation (Fig. 4). The "hypodermis preparation" (Sekizawa et al. 1999; Höger and Seyfarth 2001) has been used to study the voltage-activated conductances. The detached VS-3 organ is attached to a small coverslip that is then placed in a recording chamber and superfused with experimental solutions. The neurons are still wrapped with accessory cells, but sharp intracellular electrodes can impale the neurons to record voltage-activated conductances using the discontinuous single-electrode voltage-clamp method. Access of pharmacological agents to the neurons via superfusion is generally good, but the intracellular milieu cannot be completely changed, which limits the study of voltage-activated Na^+ and Ca^{2+} currents at strong depolarizing potentials since the K^+ currents cannot be completely blocked without replacing the intracellular K^+.

Voltage-activated K^+ and Ca^{2+} currents do not cause the different firing patterns of type A and type B neurons

Voltage-activated outward K^+ currents are important for controlling action potential duration and firing

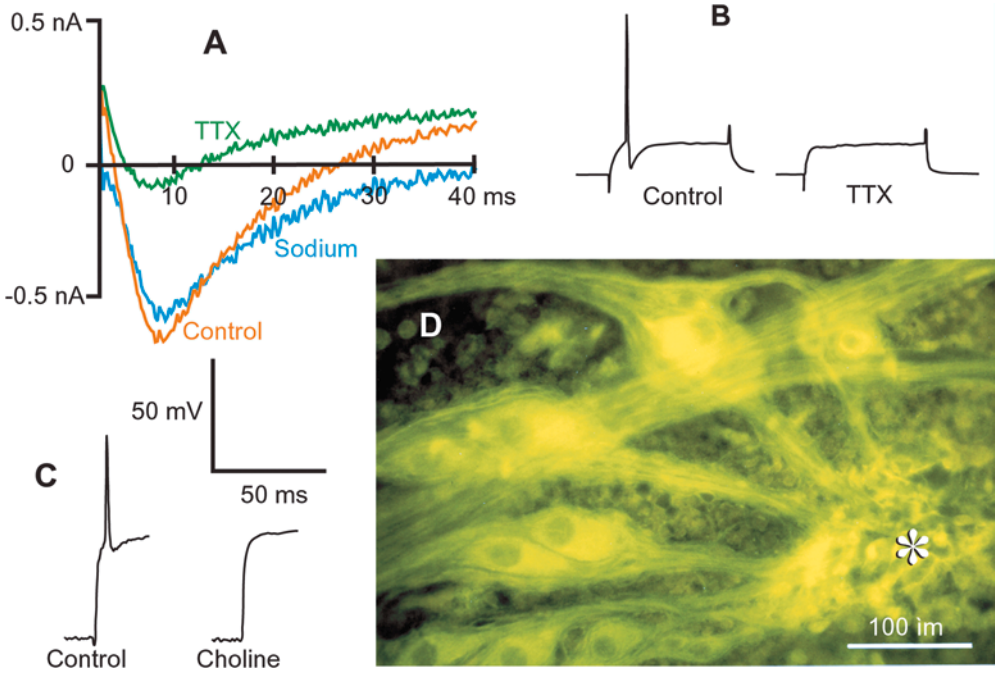

Fig. 6A–D Voltage-activated, TTX-sensitive Na^+ channels cause the action potentials in VS-3 neurons and are distributed widely in the axons, somata and dendrites. **A** Voltage-clamp steps from –90 mV to –20 mV produced an inward Na^+ current followed by an outward current due to delayed rectifier K^+ channels (*Control*). Addition of 1 μM TTX eliminated most inward current (*TTX*) and subtraction of this trace from the control revealed the voltage-activated Na^+ current. **B** Addition of 10 μM TTX eliminated action potentials produced by intracellular current injection (1 nA) into a type A neuron after 200 s. **C** Replacement of extracellular Na^+ by choline eliminated action potentials after 100 s. **D** Wholemount preparation of a VS-3 organ stained with FITC-conjugated antibody against SP19 peptide derived from the voltage-activated Na^+ channel sequence. Axons, somata and dendrites were all immunoreactive. *Asterisk* shows the dendrite tips extending to the slit region. Modified from Seyfarth and French (1994), Seyfarth et al. (1995), Torkkeli et al. (2001) and A.S. French et al., unpublished data

frequency in neurons (Hille 2001). VS-3 neurons have transient and non-inactivating K^+ currents, both of which are activated by depolarization from the resting potential (Fig. 7A; Sekizawa et al. 1999). Tetraethylammonium (TEA), 4-aminopyridine (4-AP) and quinidine blocked the transient component and they also inhibited the sustained K^+ current. These blocking chemicals increased the amplitude and duration of action potentials (Fig. 7E) but did not induce more frequent firing. This suggests that K^+ currents repolarize action potentials but do not regulate the firing rate. There was no difference in the inactivation kinetics of the transient K^+ currents of type A or type B neurons, but there was a statistically significant difference in the activation parameters of both the transient and non-inactivating components (Fig. 7B). Half-maximal activation (V_{50}) of the transient current for type B neurons was about 20 mV more negative than for type A neurons (–13.1 mV and +10.6 mV, respectively) and for the non-inactivating current this difference was about 7 mV (–56.2 mV and –48.9 mV, respectively). These differences probably reflect the fact that the type B neurons fire more action potentials at more negative potentials than type A neurons (Sekizawa et al. 1999) and therefore need a repolarizing current at more negative levels.

Ca^{2+}-activated K^+ currents [$I_{K(Ca)}$] regulate repetitive firing in many neurons (Torkkeli and French 1995). K^+ currents that could be activated by Ca^{2+} have not been identified in VS-3 neurons (Sekizawa et al. 1999) even though these neurons have a large low-voltage-activated Ca^{2+} current (LVA I_{Ca}; Fig. 7C). Outward currents were not increased if the divalent cations Cd^{2+} and Ni^{2+}, used to block the Ca^{2+} currents, were omitted from the superfusion solution and no currents were reduced by charybdotoxin, apamin or iberiotoxin, the best-known blockers of $I_{K(Ca)}$ (Sekizawa et al. 1999, 2000). Furthermore, these blocking chemicals did not change the firing behavior of VS-3 neurons. It is possible that spiders have an $I_{K(Ca)}$ with a different pharmacological profile to other neurons, or that these channels are sparse in the somatic region where most recordings were made. However, it is clear that the different firing behaviors of the two neuron types do not depend on $I_{K(Ca)}$, since I_{Ca} could be completely blocked without affecting firing frequency, action potential threshold, amplitude or duration.

The recorded LVA I_{Ca} was almost identical in type A and type B neurons (Sekizawa et al. 2000). It activated at about –45 mV and reached its maximum at about –25 mV in both neuron types (Fig. 7C, D). V_{50} values for I_{Ca} inactivation were –35.1 mV for type A and –30.3 mV for type B neurons. This difference was not statistically significant. The physiological function of I_{Ca} in VS-3 neurons is unknown. It does not regulate the firing behavior by lowering the threshold for Na^+ spikes, as reported in some vertebrate central neurons

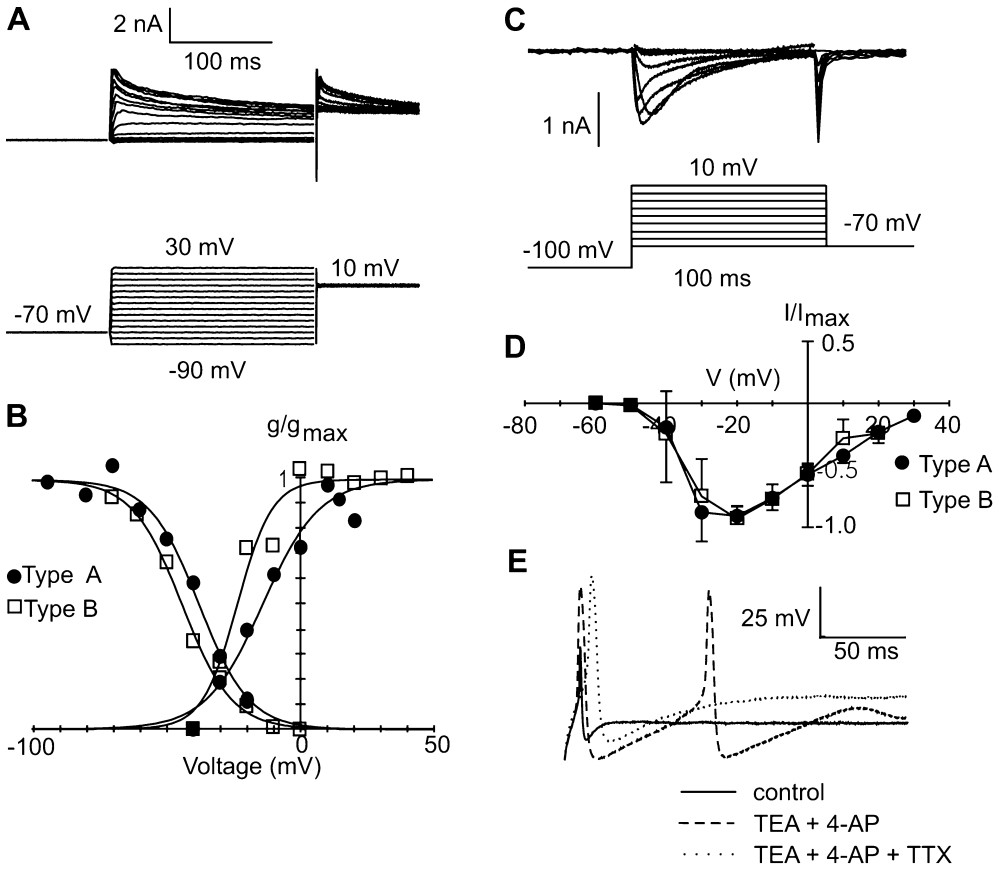

Fig. 7A–E Voltage-activated K^+ and Ca^{2+} currents in VS-3 neurons. **A** Voltage-clamp steps in a VS-3 neuron after blocking inward currents revealed two major outward K^+ currents, a non-inactivating, delayed rectifier current and a rapidly inactivating current that could be activated by depolarization from the normal resting potential. **B** Activation and inactivation parameters for the rapidly inactivating K^+ current showed that the half-maximal activation voltage (V_{50}) was higher in type A than type B neurons. A similar, but smaller, difference was found for activation of the delayed rectifier current. **C** Voltage-clamp steps after blocking Na^+ and K^+ currents revealed a low-voltage-activated Ca^{2+} current. **D** Ca^{2+} current activation was similar in type A and type B neurons. **E** Ca^{2+} current could produce action potentials with significantly higher amplitude and longer duration than the Na^+ spike when K^+ currents were blocked, and Ca^{2+} spikes were even larger when Na^+ currents were blocked. Modified from Sekizawa et al. (1999, 2000)

(Huguenard 1996). The rapid activation of I_{Ca} must increase intracellular Ca^{2+} concentration during the brief action potential, and this may allow these phasic neurons to use cellular processes that require calcium.

Inactivation properties of voltage-activated Na^+ currents control the firing patterns of type A and type B neurons

When the potassium currents were blocked, VS-3 neurons fired action potentials with larger amplitude and longer duration than normal. When Na^+ currents were blocked with TTX, the action potential became even larger and slower due to the Ca^{2+} current (Fig. 7E). Both types of neurons could only fire one "calcium spike" in response to a steady stimulus, indicating that the normal regenerative property of type B neurons can only be achieved with spikes driven by a rapidly inactivating I_{Na}. Kinetic study of I_{Na} was restricted to situations where extracellular Na^+ concentration was reduced to about half the physiological value. The V_{50} values for I_{Na} were about –30 mV in both neuron types (Torkkeli et al. 2001). However, the inactivation properties of I_{Na} were different in the two neuron types with V_{50} of –40.1 mV in type A neurons and –58.1 mV in type B neurons (Fig. 8A). The slope factors of the inactivation curves were also different: 6.8 mV and 9.3 mV, respectively. In addition, there was a significant difference in the ability of the I_{Na} to recover from inactivation after being activated (Fig. 8B; Torkkeli et al. 2001). While recovery from inactivation was faster at more negative potentials, it was always slower in type A than in type B neurons (Fig. 8B).

Information from voltage-clamp measurements was used to simulate the different firing patterns in the two neurons using a simplified Hodgkin-Huxley model to test the effect of different currents on firing behavior (Torkkeli and French 2002). Changing only two parameters of Na^+ current inactivation, the slope of the inactivation curve (h_4) and the time-constant of recovery from inactivation (τ_{max}) (Fig. 8C, D) converted the model from firing single spikes into firing bursts of action potentials (Fig. 8E). These results indicate that Na^+ channel inactivation controls the firing properties of the VS-3 neurons, and that changing only two parameters of inactivation can achieve a complete transformation between the two neuron types.

Frequency response functions and information capacities in VS-3 neurons

The two types of VS-3 neurons respond very differently to step mechanical or electrical stimulation, but natural stimuli are likely to be more random or possibly rhythmic. With oscillatory stimuli the responses of the two neuron types tended to be more similar, with both

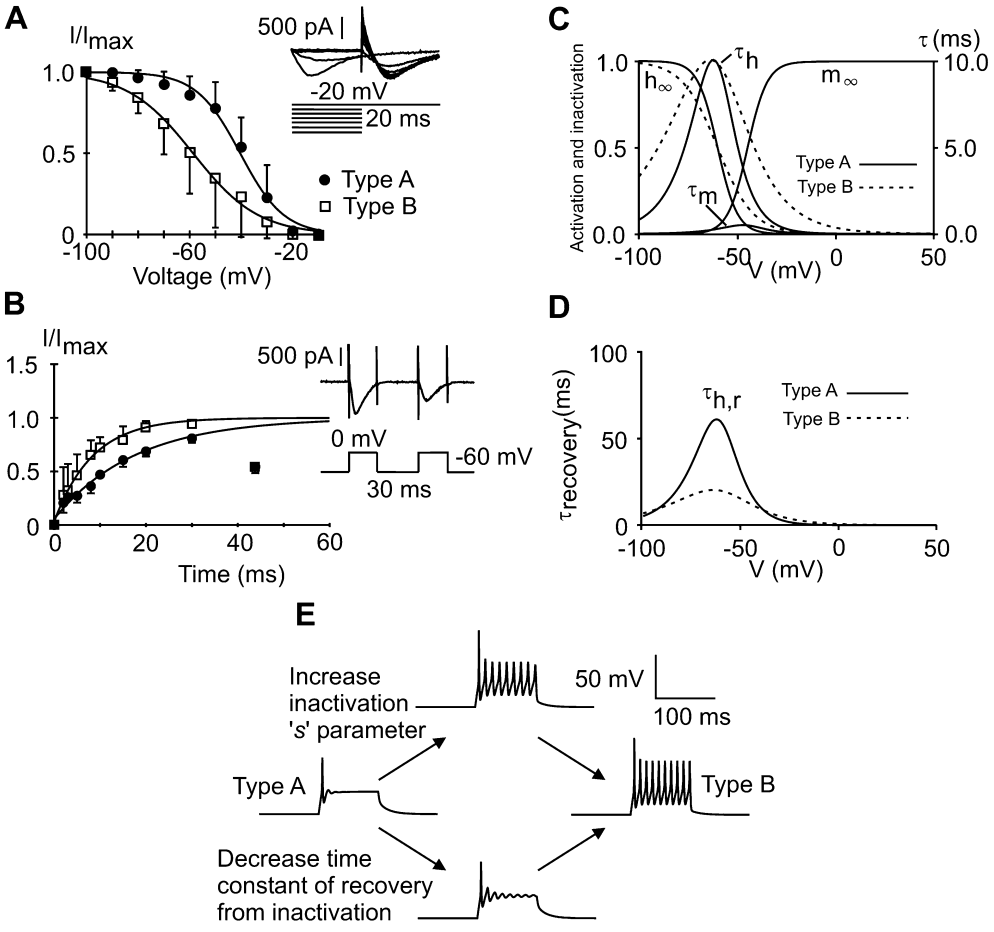

Fig. 8A–E The different firing patterns in type A and type B neurons can be explained by differences in the inactivation properties of voltage-activated Na^+ currents. Voltage-activated Na^+ currents had different inactivation properties, primarily in their slope (*s*) factors (**A**) and their time-constants of recovery from inactivation (**B**). Firing patterns in the two neurons types were simulated by a simple model containing only voltage-activated Na^+ and K^+ (delayed rectifier) ion channels. Kinetic parameters of the model ion channels differed in the slope of activation, which also changed the time-constant (**C**), and in the time-constant of recovery from inactivation (**D**). **E** Changing these two parameters allowed a complete transition from type A to type B firing. Modified from Torkkeli et al. (2001) and Torkkeli and French (2002)

neurons able to follow sinusoidal current injections at more than 100 Hz (Seyfarth and French 1994). Broadband stimulation gave high-pass frequency responses that could be described by the power-law relationship:

$$G(f) = Af^k \tag{3}$$

where $G(f)$ is the amplitude of the gain as a function of frequency, f; A and k are constants. This relationship was found in both neuron types, and with both mechanical (Fig. 9A) and electrical (Fig. 9B) stimulation. The power-law relationship has been seen in a wide variety of sensory systems (Thorson and Biederman-Thorson 1974) including other lyriform organs of *C. salei* (Bohnenberger 1981) and its basis is unknown, although some evidence suggests that it is due to the presence of multiple adaptation processes with a range of exponential time constants (French and Torkkeli 1994). The frequency exponent, k, was significantly higher in type A than in type B neurons (0.39 versus 0.24 for mechanical stimulation) indicating that type A neurons respond better to rapid inputs than type B neurons over a wide range of stimulus conditions.

The ability to observe the receptor current and potential in VS-3 neurons offers the possibility of measuring how information is encoded at each stage

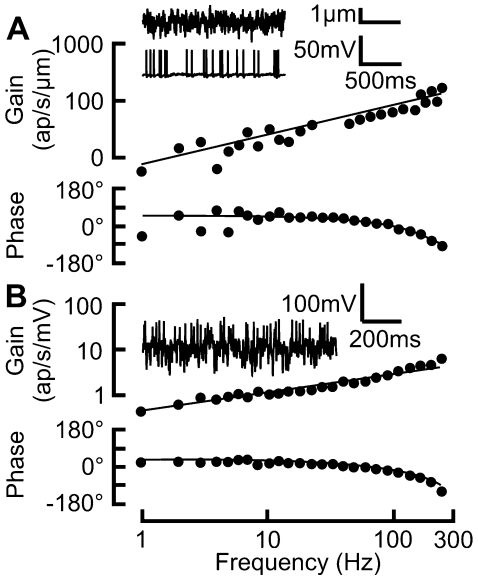

Fig. 9A,B Frequency response functions of VS-3 neurons follow a power-law model for both mechanical and electrical stimulation. **A** Bode plot of frequency response obtained by random mechanical stimulation (*inset* shows sample of raw data) fitted by a power law (Eq. 3) with exponent $k = 0.37$ and a delay $\tau = 0.85$ ms (*solid lines*). **B** Bode plot for intracellular electrical stimulation fitted by $k = 0.39$ and $\tau = 1.41$ ms. Modified from French et al. (2001)

of the mechanoreceptor process, from stimulus through transduction to action potential encoding. Measures of information transmission at each stage indicated that during normal transduction, when the receptor current produces a receptor potential, it interacts with the voltage-activated conductances to give a better signal-to-noise ratio than would be observed from the current alone at a constant membrane potential. However, conversion of the receptor potential into action potentials dramatically reduced the available information capacity, as found in other systems (Juusola and French 1997). Information capacity in the two neuron types was similar (French et al. 2001).

Modulation of VS-3 neurons by efferent innervation and peripheral inhibition

Efferent neurotransmitter candidates

Immunolabeling with a polyclonal antiserum against the neuronal transmitter GABA demonstrated that the VS-3 neurons receive GABA-like immunoreactive (GABA-LIR) fibers (Fig. 10A). However, double immunolabeling with the vesicle protein synapsin indicated that not all presynaptic sites exhibit GABA-LIR (Fabian-Fine et al. 1999b). This result was confirmed by immuno-EM; only some presynaptic profiles were labeled against GABA (Fabian-Fine et al. 2000). There are at least three different GABA-LIR fiber types, thick, medium, and thin, each with characteristic size and spacing of the varicosities (Fig. 10B–D). Light (LM) and electron (EM) microscopic immunolabeling showed that glutamate is another transmitter candidate in VS-3. Fine glutamate-LIR fibers formed numerous varicosities along the sensory neurons, but there was no evidence for several distinct fiber types, as for GABA-LIR fibers. The specificity of immunostaining was supported by the presence of immunoreactivity against kainate-type glutamate receptors (GluR 5,6,7; Fabian-Fine et al. 2000). The situation is summarized in Fig. 2A.

A possible additional neurotransmitter at peripheral synapses is ACh, the principal excitatory afferent transmitter of mechanosensory neurons in arthropods and a transmitter candidate in the sensory neurons of slit sense organs and tactile hairs of spiders (Fabian and

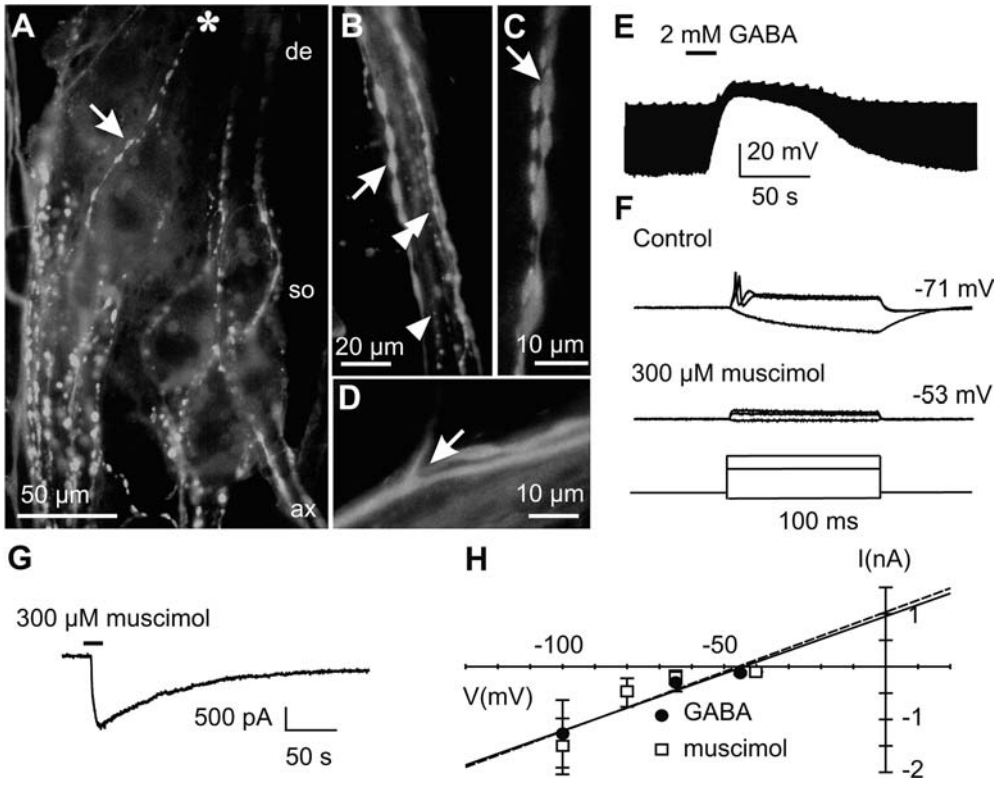

Fig. 10A–H GABAergic modulation of VS-3 neurons. **A** Whole-mount preparation labeled with fluorochrome Cy3 showed GABA-immunoreactive fibers and varicosities (*arrow*) extending across the axonal (*ax*), somatic (*so*), and dendritic (*de*) regions of the neurons (*asterisk*: dendrite tips extending towards the slit region). **B** Initial axon segment, demonstrating three types of immunoreactive fibers and varicosities: thick (*arrow*), medium (*double arrowhead*), and thin (*single arrowhead*). **C** Two GABA-immunoreactive fibers (thick and medium) at higher magnification forming serial varicosities (*arrow*) next to each other. **D** Branching immunoreactive fiber in axonal region of VS-3 neurons. **E** GABA applied to a VS-3 neuron caused depolarization and increased membrane conductance, as shown by the response to repetitive intracellular current pulses. **F** GABA, and an agonist of ionotropic GABA receptors, muscimol, caused a complete and reversible blockade of action potentials. **G** Under voltage-clamp at –100 mV, muscimol produced an inward current. **H** The GABAergic current reversed at –45 mV, close to the Cl^- equilibrium potential. Modified from Fabian-Fine et al. (1999b) and Panek et al. (2002)

Seyfarth 1997). Immunolabeling for ChAT revealed distinct punctate immunoreactivity not only in the somata of the sensory neurons, which are probably cholinergic (Fabian and Seyfarth 1997), but also arranged linearly and with similar sizes and locations to those seen with anti-synapsin staining, but less frequent (Fabian-Fine et al. 2002).

Types of synaptic contact

A systematic examination of the ultrastructure of the various synaptic contacts encountered along VS-3 neurons showed that at least four types exist, primarily based on distinct presynaptic vesicle populations (Fabian-Fine et al. 2000). Type 1 synapses contain small, spherical, electron-lucent vesicles with a mean diameter of 32 nm (Fig. 2C). The GABA-LIR synapses and possibly the anti-ChAT varicosities mentioned above are type 1 synapses. Type 2 synapses have a population of larger spherical, electron-lucent vesicles with a mean diameter of 42 nm; EM immunolabeling evidence showed that these vesicles may contain glutamate. Type 3 synapses are characterized by a mixed vesicle population of small and large spherical electron-lucent vesicles plus dense-core and/or granular vesicles. Type 4 synapses contain a distinct population of large electron-lucent vesicles with a diameter between 37 and 65 nm. So far it is not clear what neurotransmitters may be used by type 3 and type 4 synapses.

Synaptic contacts do not form exclusively between efferent fibers and the sensory neurons, but also between the efferent fibers themselves; they even involve glial cells. There are abundant conventional monadic synapses and numerous dyad complexes. Monadic contacts form at sensory neurons, efferent fibers and glial cells, and involve all four synapse types listed above. In dyadic synapses a single presynaptic element abuts various pairs of postsynaptic elements in different combinations of sensory neuron, efferent fiber and glial cell. Reciprocal synapses, as well as serial and convergent contacts, have also been identified. These ultrastructural results have recently been summarized by Fabian-Fine et al. (2002) and compared with the situation in crustacean muscle receptor organs, which receive similar efferent innervation in the periphery. Taken together, the immense diversity of these multiple synaptic contacts and their transmitters provides extensive neuronal microcircuits for signal modulation at different levels. One case, the peripheral GABAergic inhibition of the electrical excitability of VS-3 neurons, is discussed below.

Peripheral GABAergic inhibition

Bath application of GABA or muscimol, agonists of ionotropic GABA receptors, induced a depolarization in VS-3 neurons, similar to the primary afferent depolarization (PAD) that has been described in the afferent terminals of many mechanosensory neurons (Fig. 10E; Panek et al. 2002). This depolarization occurs in the VS-3 somata where it inhibits neuronal excitability (Fig. 10F). GABA application caused a significant increase, or "shunting", in the membrane conductance (Fig. 10E, F), a common feature of GABAergic inhibition in many other neurons. The GABA- or muscimol-induced current was inward at potentials below –45 mV (Fig. 10G, H). It could be blocked by the Cl^- current blocker picrotoxin but was insensitive to bicuculline, a blocker of vertebrate $GABA_A$ receptors. The Hill coefficient of the GABA-induced current was 1.6, indicating that one or two binding sites are needed for channel opening, and the GABA concentration at half maximal current (EC_{50}) was 103.4 μM (Panek et al. 2002). These findings are close to those previously described for *Drosophila* GABA receptors (Hosie et al. 2001) and for vertebrate $GABA_A$ receptors (Bormann 2000).

GABA-induced inhibition has been attributed to two main mechanisms: depolarization-induced inactivation of I_{Na} (Zhang and Jackson 1995) or membrane shunting (Cattaert and El Manira 1999). In VS-3 neurons the inhibition can be completely explained by membrane shunting, because the neurons did not fire in the presence of GABA, even when held at the resting potential where Na^+ channels would not have been inactivated (Panek et al. 2002).

Since GABAergic inhibition in the periphery suppresses impulse propagation to all axonal branches, it will allow rapid adjustment of the behavioral responses to changing situations by selecting the signals to be carried to the CNS. This could give spiders a mechanism for rapidly distinguishing between signals from background vibrations, locomotor movements, potential prey, predators or mates.

Conclusions, questions and future directions

A useful goal for slit sense organ research would be to create a theoretical model of a functioning slit and its associated neurons that could faithfully reproduce the response to any mechanical stimulus. Such a model would not only be useful for testing and proving our understanding of the various components of the receptors, but could also have important consequences in fields such as prosthetics and robotics. Current knowledge can be assessed in the context of this goal, taking each of the principal stages in turn.

The general structure and ultrastructure of the slits are fairly clear, but we know little about the mechanical properties of the components that connect the slits to the dendritic membranes. Detailed studies of the materials involved, followed by careful computer simulations would provide useful information. The mechanical structures could contribute significantly to the time-dependent properties of the receptors, although this does not seem to be as important as the electrical properties of the neuronal membranes. The functional significance

of the different morphologies of the two sensory dendrites in VS-3 is a puzzle, which might be resolved by a better understanding of the slit mechanics, as well as more thorough descriptions of the relationship between neuron type (A or B) and ultrastructure.

The molecular biology of the mechanically activated ion channels presents a major challenge. Transduction probably only involves a few hundred of these molecules in each cell, and their location is relatively inaccessible. It is possible that work on other systems will provide new molecular tools for this problem, such as specific antibodies or oligonucleotides, but the way ahead is not yet clear.

Beyond the primary step of transduction, electrical activity spreads through the neurons until action potentials are produced. The excitability of different neuronal regions, and the relative contributions of decremental and regenerative processes to overall electrical behavior, are important questions that have never been settled satisfactorily in any cuticular sensilla but which may be resolved by applying a range of techniques such as imaging of ion- or voltage-sensitive dyes, or molecular labeling of ion channels.

The major voltage-activated ion channels are now known, although their detailed contributions to complete firing patterns must be more thoroughly investigated. The role of the calcium current is particularly enigmatic, and deserves more experimental work to study the effects of blocking or enhancing calcium entry on long-term neuronal function. It is also possible that ion channels, including the mechanically activated channels, are modulated by second-messenger molecules, including calcium.

Efferent innervation of spider mechanoreceptors raises a number of questions, including the identification of the various transmitters involved, the functional roles of the different types of synapses and receptors, interactions between the different efferent pathways, as well as the origins and the functions of the efferent neurons themselves. Voltage clamp of VS-3 neurons, combined with pharmacology, is likely to be very useful here.

Finally, although much neuroanatomical work has already been performed on lyriform organs (as reviewed in detail by Barth 2001), the central projections and functions of the VS-3 afferents themselves are not yet mapped or understood. While these are not essential to building a functional simulation of the organs, they are crucially important to understanding why these receptors are constructed in such a complex and interesting manner.

Acknowledgements We are grateful to Ruth Fabian-Fine, Ulli Höger, Mikko Juusola, Izabela Panek and Shin-ichi Sekizawa for all their contributions to the work described here. Support was provided by grants from the Canadian Institutes of Health Research to A.S.F. and P.H.T., The Natural Engineering and Sciences Council of Canada to P.H.T., the Deutsche Forschungsgemeinschaft to E.-A.S., and a Collaborative Research Grant from NATO.

References

Barth FG (1971) Der sensorische Apparat der Spaltsinnesorgane (*Cupiennius salei* Keys, Araneae). Z Zellforsch 112:212–246

Barth FG (1972a) Die Physiologie der Spaltsinnesorgane. I. Modellversuche zur Rolle des cuticularen Spaltes beim Reiztransport. J Comp Physiol 78:315–336

Barth FG (1972b) Die Physiologie der Spaltsinnesorgane. II. Funktionelle Morphologie eines Mechanoreceptors. J Comp Physiol 81:159–186

Barth FG (1985) Slit sensilla and the measurement of cuticular strains. In: Barth FG (ed) Neurobiology of arachnids. Springer, Berlin Heidelberg New York, pp 162–188

Barth FG (2001) A spider's world. Senses and behavior. Springer, Berlin Heidelberg New York

Barth FG, Libera W (1970) Ein Atlas der Spaltsinnesorgane von *Cupiennius salei* Keys. Chelicerata (Araneae). Z Morphol Tiere 68:343–369

Bohnenberger J (1981) Matched transfer characteristics of single units in a compound slit sense organ. J Comp Physiol A 142:391–402

Bormann J (2000) The "ABC" of GABA receptors. Trends Pharmacol Sci 21:16–19

Cattaert D, El Manira A (1999) Shunting versus inactivation: Analysis of presynaptic inhibitory mechanisms in primary afferents of the crayfish. J Neurosci 19:6079–6089

Fabian R, Seyfarth E-A (1997) Acetylcholine and histamine are transmitter candidates in identifiable mechanosensitive neurons of the spider *Cupiennius salei*: an immunocytochemical study. Cell Tissue Res 287:413–423

Fabian-Fine R, Volknandt W, Seyfarth E-A (1999a) Peripheral synapses at identifiable mechanosensory neurons in the spider *Cupiennius salei*: synapsin-like immunoreactivity. Cell Tissue Res 295:13–19

Fabian-Fine R, Höger U, Seyfarth E-A, Meinertzhagen IA (1999b) Peripheral synapses at identified mechanosensory neurons in spiders: three-dimensional reconstruction and GABA immunocytochemistry. J Neurosci 19:298–310

Fabian-Fine R, Meinertzhagen IA, Seyfarth E-A (2000) Organization of efferent peripheral synapses at mechanosensory neurons in spiders. J Comp Neurol 420:195–210

Fabian-Fine R, Seyfarth E-A, Meinertzhagen IA (2002) Peripheral synaptic contacts at mechanoreceptors in arachnids and crustaceans: morphological and immunocytochemical characteristics. Microsc Res Tech 58:283–298

Foelix RF (1975) Occurrence of synapses in peripheral sensory nerves of arachnids. Nature 254:146–148

French AS (1988) Transduction mechanisms of mechanosensilla. Annu Rev Entomol 33:39–58

French AS, Torkkeli PH (1994) The time-course of sensory adaptation in the cockroach tactile spine. Neurosci Lett 178 :147–150

French AS, Höger U, Sekizawa S-I, Torkkeli PH (2001) Frequency response functions and information capacities of paired spider mechanoreceptor neurons. Biol Cybern 85:293–300

Grünert U, Gnatzy W (1987) K^+ and Ca^{2+} in the receptor lymph of arthropod cuticular receptors. J Comp Physiol A 161:329–333

Hille B (2001) Ionic channels of excitable membranes. Sinauer, Sunderland, MA

Höger U, French AS (1999a) Estimated single-channel conductance of mechanically-activated channels in a spider mechanoreceptor. Brain Res 826:230–235

Höger U, French AS (1999b) Temperature sensitivity of transduction and action potential conduction in a spider mechanoreceptor. Pflügers Arch 438:837–842

Höger U, Seyfarth E-A (2001) Structural correlates of mechanosensory transduction and adaptation in identified neurons of spider slit sensilla. J Comp Physiol A 187:727–736

Höger U, Torkkeli PH, Seyfarth E-A, French AS (1997) Ionic selectivity of mechanically activated channels in spider mechanoreceptor neurons. J Neurophysiol 78:2079–2085

Hosie AM, Buckingham SD, Presnail JK, Sattelle DB (2001) Alternative splicing of a *Drosophila* GABA receptor subunit gene identifies determinants of agonist potency. Neuroscience 102:709–714

Huguenard JR (1996) Low-threshold calcium currents in central nervous system neurons. Annu Rev Physiol 58:329–348

Juusola M, French AS (1997) The efficiency of sensory information coding by mechanoreceptor neurons. Neuron 18:959–968

Juusola M, French AS (1998) Adaptation properties of two types of sensory neurons in a spider mechanoreceptor organ. J Neurophysiol 80:2781–2784

Juusola M, Seyfarth E-A, French AS (1994) Sodium-dependent receptor current in a new mechanoreceptor preparation. J Neurophysiol 72:3026–3028

Juusola M, Seyfarth E-A, French AS (1997) Rapid coating of glass-capillary microelectrodes for single-electrode voltage-clamp. J Neurosci Methods 71:199–204

McIver SB (1985) Mechanoreception. In: Kerkut GA, Gilbert LI (eds) Comprehensive insect physiology, biochemistry and pharmacology. Pergamon Press, Oxford, pp 71–132

Morris CE (2001) Mechanosensitive ion channels in eukaryotic cells. In: Sperelakis N (ed) Cell physiology sourcebook – a molecular approach. Academic Press, San Diego, pp 745–760

Panek I, French AS, Seyfarth E-A, Sekizawa S-I, Torkkeli PH (2002) Peripheral GABAergic inhibition of spider mechanosensory afferents. Eur J Neurosci 16:96–104

Polder HR, Swandulla D (2001) The use of control theory for the design of voltage clamp systems: a simple and standardized procedure for evaluating system parameters. J Neurosci Methods 109:97–109

Rick R, Pawel AV (1976) X-ray microanalysis of receptor lymph in a cuticular arthropod sensillum. J Comp Physiol 110:89–95

Sekizawa S-I, French AS, Höger U, Torkkeli PH (1999) Voltage-activated potassium outward currents in two types of spider mechanoreceptor neurons. J Neurophysiol 81:2937–2944

Sekizawa S-I, French AS, Torkkeli PH (2000) Low-voltage-activated calcium current does not regulate the firing behavior in paired mechanosensory neurons with different adaptation properties. J Neurophysiol 83:746–753

Seyfarth E-A, French AS (1994) Intracellular characterization of identified sensory cells in a new spider mechanoreceptor preparation. J Neurophysiol 71:1422–1427

Seyfarth E-A, Bohnenberger J, Thorson J (1982) Electrical and mechanical stimulation of a spider slit sensillum: outward current excites. J Comp Physiol A 147:423–432

Seyfarth E-A, Sanders EJ, French AS (1995) Sodium channel distribution in a spider mechanosensory organ. Brain Res 683:93–101

Thorson J, Biederman-Thorson M (1974) Distributed relaxation processes in sensory adaptation. Science 183:161–172

Torkkeli PH, French AS (1995) Slowly inactivating outward currents in a cuticular mechanoreceptor neuron of the cockroach (*Periplaneta americana*). J Neurophysiol 74:1200–1211

Torkkeli PH, French AS (2002) Simulation of different firing patterns in paired spider mechanoreceptor neurons: the role of Na^+ channel inactivation. J Neurophysiol 87:1363–1368

Torkkeli PH, Sekizawa S-I, French AS (2001) Inactivation of voltage-activated Na^+ currents contributes to different adaptation properties of paired mechanosensory neurons. J Neurophysiol 85:1595–1602

Traynelis SF, Jaramillo F (1998) Getting the most out of noise in the central nervous system. Trends Neurosci 21:137–145

Vassilev PM, Scheuer T, Catterall WA (1989) Inhibition of inactivation of single sodium channels by a site-directed antibody. Proc Natl Acad Sci USA 86:8147–8151

Yang X, Sachs F (1989) Block of stretch-activated ion channels in *Xenopus* oocytes by gadolinium and calcium ions. Science 243:1068–1071

Zhang SJ, Jackson MB (1995) Properties of the $GABA_A$ receptor of rat posterior pituitary nerve terminals. J Neurophysiol 73:1135–1144